Applied Environmental Biotechnology

Research Article

Amadori-assisted hydrothermal synthesis of blue-luminescent glucose-derived graphene quantum dot dispersion for smartphone-assisted fluorescence screening of *Staphylococcus aureus*

Siti Nor Hadijah Zalriadi, Siti Aisyah Saiful Adlee, Wan Hazman Danial*, Mohammad Norazmi Ahmad

Department of Chemistry, Kulliyyah of Science, International Islamic University Malaysia, 25200 Kuantan, Pahang, Malaysia

Abstract

Rapid bacterial detection requires inexpensive fluorescent probes compatible with portable readout. Herein, a blue-luminescent graphene quantum dots (GQDs) dispersion was synthesized through a bottom-up hydrothermal route using glucose as the carbon precursor, hexadecylamine as the nitrogen source, and acetic acid to promote Amadori-rearrangement-assisted carbonization. The resulting pale-yellow solution emitted intense blue fluorescence under ultraviolet irradiation. Attenuated total reflectance–Fourier transform infrared spectroscopy confirmed surface amine, hydroxyl/oxygenated, aromatic C=C, C–O, C–O–C, and epoxide-related groups, indicating functionalized carbon nanostructures suitable for biological interactions. UV-Vis spectroscopy showed absorption bands at 205 and 257 nm, assigned to π–π* transitions of sp^2 carbon domains, and a shoulder near 340 nm attributed to n–π* transitions of carbonyl/oxygenated groups. Dynamic light scattering reported an average hydrodynamic diameter of 44.20 nm, whereas transmission electron microscopy revealed predominantly spherical particles with sizes of 10–70 nm and an estimated mean diameter of 33.69 nm. The GQDs were evaluated as turn-off fluorescent probes for *Staphylococcus aureus* using smartphone-based RGB analysis. Fluorescence quenching increased with bacterial/GQD concentration, producing a linear RGB response (R^2 = 0.8218) and a Stern–Volmer-type correlation (R^2 = 0.9201). These findings support glucose-derived GQDs as low-cost nanoprobes for preliminary portable bacterial screening, although further validation using calibrated colony-forming unit levels, selectivity, and real matrices remains necessary.

Keywords: Graphene quantum dots; Amadori rearrangement; Glucose; Fluorescence quenching; *Staphylococcus aureus*

***Corresponding author:**
Wan Hazman Danial
(whazman@iium.edu.my)

Citation: Zalriadi, S. N. H., Adlee, S. A. S., Danial, W. H., & Ahmad, M. N. Amadori-assisted hydrothermal synthesis of blue-luminescent glucose-derived graphene quantum dot dispersion for smartphone-assisted fluorescence screening of *Staphylococcus aureus*. *Appl Environ Biotechnol*. http://doi.org/10.26789/AEB.2026.01.004

Received: November 9, 2026

Revised: November 17, 2026

Accepted: November 17, 2026

Published online: November 25, 2026

Copyright: © 2026 Author(s). This is an Open-Access article distributed under the terms of the Creative Commons Attribution License, permitting distribution, and reproduction in any medium, provided the original work is properly cited.

Publisher's Note: AccScience Publishing remains neutral with regard to jurisdictional claims in published maps and institutional affiliations.

1. Introduction

Staphylococcus aureus is one of the most clinically and environmentally important opportunistic bacterial pathogens because it can colonize humans and animals without symptoms while also causing diseases ranging from superficial skin infection to necrotizing fasciitis, endocarditis, osteomyelitis, bloodstream infection, and food

poisoning (Girma, 2025; Haag *et al.*, 2019; Mlynarczyk-Bonikowska & Rudnicka, 2025). Its significance is amplified by toxin production, quorum-sensing-mediated virulence, and the capacity to develop antibiotic resistance, which collectively make rapid detection important for clinical, food-safety, and environmental monitoring (Moellering, 2010; Z. Zhu *et al.*, 2024). Culture-based methods remain important for confirmation, but they are slow, labor-intensive, and poorly suited for immediate screening; some approaches also struggle with viable-but-non-culturable cells and therefore may delay decision-making (Kalkal *et al.*, 2020; Šuster & Cör, 2023; Zhao *et al.*, 2024).

Biosensor technologies offer a route to faster pathogen detection because the target recognition event can be converted directly into an optical, electrochemical, or photoelectrochemical signal (Awaludin *et al.*, 2020; Jiang *et al.*, 2021; Savas & Altintas, 2019). Among optical nanoprobes, graphene quantum dots (GQDs) are attractive because they combine nanoscale carbon domains, high surface-to-volume ratio, tunable photoluminescence, photostability, water dispersibility, and low toxicity (Bressi *et al.*, 2021; Elvati *et al.*, 2017; Kwon *et al.*, 2022; Wijayaratne *et al.*, 2022). Their fluorescence is generally associated with quantum confinement, edge states, surface defects, and surface functional groups such as hydroxyl, carboxyl, carbonyl, epoxy, and amine groups (Kalluri *et al.*, 2018; Shebeeb *et al.*, 2022; S. Zhu *et al.*, 2015; S. Zhu *et al.*, 2017). These surface groups also create opportunities for interaction with bacterial envelopes or with recognition ligands, enabling fluorescence quenching or enhancement strategies for bacterial detection (Bruce & Clapper, 2020; Dehghani *et al.*, 2020; Li *et al.*, 2025).

Graphene quantum dots can be synthesized using top-down or bottom-up methods. Top-down routes cleave larger carbon materials such as graphite, graphene, or carbon nanotubes into nanoscale domains, but they often require aggressive oxidation, extensive purification, and may produce broad size distributions and structural defects (Chen *et al.*, 2018; Rasheed *et al.*, 2024; Sun *et al.*, 2023). Bottom-up synthesis assembles carbon dots from small molecular precursors through dehydration, condensation, aromatization, carbonization, and passivation reactions, allowing better control over precursor chemistry and surface functionalization (Shi *et al.*, 2023; Y. Wang *et al.*, 2025). Green bottom-up synthesis using biomass-derived or low-toxicity precursors is particularly attractive because it reduces reliance on harsh reagents while producing fluorescent carbon nanomaterials suitable for biosensing (Bressi *et al.*, 2021; Padmavathi & Vijayakumar, 2023).

Glucose is a useful carbon source because it is inexpensive, renewable, water-compatible, and reactive under hydrothermal conditions (Mielewczyk *et al.*, 2025). In the presence of amine-containing compounds, reducing sugars can participate in Maillard-type chemistry involving glycosylamine formation and Amadori rearrangement, generating nitrogen-containing intermediates that promote the formation of heterocyclic and aromatic carbonaceous structures (Cho *et al.*, 2024; Zhang *et al.*, 2022). In this study, a blue-luminescent glucose-derived GQD dispersion was prepared using an Amadori-assisted hydrothermal route with hexadecylamine as the nitrogen source and acetic acid as the rearrangement promoter. The resulting GQDs were purified through cold-induced aggregation and characterized in terms of surface functionality, optical absorption behavior, hydrodynamic particle-size distribution, and nanoscale morphology using attenuated total reflectance–Fourier transform infrared spectroscopy (ATR-FTIR), UV-Vis spectroscopy, dynamic light scattering (DLS), and transmission electron microscopy (TEM). The dispersion was further evaluated as a smartphone-readable fluorescent probe for *S. aureus* screening based on fluorescence quenching and RGB analysis. By combining simple precursor chemistry, colloidal nanomaterial characterization, cold-aggregation purification, and portable fluorescence readout, this work positions glucose-derived GQDs as a low-cost dispersion-based fluorescent platform for bacterial screening.

2. Experimental section

2.1. Materials

Glucose (HmbG Chemicals, Germany) was used as the carbon precursor. Hexadecylamine (Merck Millipore, Germany) served as the nitrogen source, glacial acetic acid (QRëC, New Zealand) was used to facilitate the Amadori rearrangement, and hexanol (QRëC) was used to dissolve hexadecylamine. Deionized water was used throughout the synthesis and dilution steps. Methanol (R&M Chemicals, Malaysia) was used for purification, and phosphate-buffered saline (PBS; Vivantis, Malaysia) was used for washing bacterial samples.

2.2. Synthesis of graphene quantum dots

The GQDs were synthesized using a bottom-up hydrothermal method adapted from glucose-derived carbon-dot chemistry. First, 0.1 g glucose was dissolved in 1 mL deionized water with stirring, followed by the addition of 200 µL glacial acetic acid. Separately, 0.8 g hexadecylamine was dissolved in 10 mL warm hexanol at 60 °C to ensure complete dissolution. The hexadecylamine solution was then added slowly to the glucose–acetic acid solution under continuous stirring to obtain a homogeneous precursor suspension.

The suspension was transferred into a Teflon-lined stainless-steel autoclave. Nitrogen gas was purged into the autoclave for 15 min before sealing to minimize unwanted oxidation during the hydrothermal reaction. The sealed autoclave was heated at 160 °C for 4 h to promote dehydration, condensation, aromatization, and carbonization of the precursors (Cho *et al.*, 2024; Qu *et al.*, 2014). After the reaction, the autoclave was allowed to cool naturally to room temperature for approximately 2 h before opening.

2.3. Purification

The reaction was terminated by blending the product mixture with 290 mL methanol, followed by bath sonication for 1 h. Residual aliphatic amines were removed using cold-induced aggregation: the mixture was stored at −25 °C to −35 °C for more than 3 h, after which the precipitated impurities were removed using vacuum filtration through a 0.22 μm polyvinylidene fluoride (PVDF) membrane. The filtrate was a homogeneous transparent pale-yellow solution that emitted blue fluorescence under ultraviolet irradiation, consistent with successful formation of fluorescent GQDs (Lee *et al.*, 2019; Rosato *et al.*, 2024).

2.4. Characterization

The ATR-FTIR analysis was performed using a PerkinElmer Frontier FTIR spectrometer (United States of America [USA]) to identify surface functional groups. Because the GQDs were obtained in liquid form, the sample was freeze-dried at −70 °C before ATR-FTIR measurement. Spectra were collected over 400–4000 cm^{-1} and interpreted by comparison with literature assignments.

The UV-Vis absorption spectra were recorded using a Shimadzu UV-1900i spectrophotometer (Japan) from 200 to 500 nm. The GQD solution was diluted with methanol at a 1:100 ratio before measurement. DLS analysis was carried out using Nano-ZS particle size analyzer Malvern instrumentation (United Kingdom) after the GQD solution was ultrasonicated for 2.5 h at 50% amplitude and diluted with deionized water at a 1:1000 ratio to reduce multiple scattering and aggregation effects (Azimi *et al.*, 2024). TEM was performed using a Thermo Fisher Talos microscope (USA) at 120 kV. The GQD dispersion was diluted with ethanol, sonicated for 15 min, drop-cast on a copper grid, and dried before imaging. Particle diameters were estimated from TEM images using ImageJ (National Institutes of Health, USA) (Danial *et al.*, 2022).

2.5. Fluorescence sensing of *Staphylococcus aureus*

Staphylococcus aureus was cultured on agar plates at 37 °C for 24 h and then subcultured in Luria-Bertani broth for an additional 24 h. The liquid culture was centrifuged at 4,000 rpm for 10 min to harvest bacterial cells and remove the growth medium. The bacterial cells were mixed with GQD samples at nominal test concentration levels of 0.1 M, 0.5 M, 1.0 M, and 1.5 M as prepared in the protocol, incubated at 37 °C for 1 h, centrifuged at 4,000 rpm for 10 min to collect bacteria–GQD complexes, washed with PBS (pH 7.4), and centrifuged again to remove unbound GQDs (Roh *et al.*, 2019).

Fluorescence response was evaluated using a smartphone-assisted digital image method. Samples were placed under a UV viewing cabinet with 254 nm excitation and imaged at a fixed camera distance under identical lighting conditions. Red (R), green (G), and blue (B) channel intensities were extracted using image-processing/color-picker software (Color Meter), and the R/(G+B) ratio was used for quantitative comparison because ratio-based analysis can reduce background and illumination variation (Fu *et al.*, 2024; Liu *et al.*, 2024; Mohammad Ameen *et al.*, 2025). Fluorescence quenching was further evaluated using the relative F_0/F response, where F_0 and F represent fluorescence-related digital intensity before and after interaction with *S. aureus*, respectively.

3. Results and discussion

3.1. Formation of glucose-derived GQDs through Amadori-rearrangement-assisted hydrothermal chemistry

The synthesis produced a homogeneous pale-yellow filtrate that emitted blue fluorescence under UV irradiation. The visual appearance after purification is important because unreacted amine-rich by-products and large carbonized aggregates would be expected to cause turbidity, precipitation, or unstable optical response. The formation route is consistent with Maillard-type chemistry: glucose first condenses with the amine functionality of hexadecylamine to form N-substituted glycosylamine intermediates, followed by Amadori rearrangement to ketosamine structures, dehydration, fragmentation, and the formation of furfurals, aldehydes, aldols, N-free polymers, and nitrogen-containing heterocycles such as pyridines, pyrazines, and pyrroles (Cho *et al.*, 2024; Zhang *et al.*, 2022). Under hydrothermal conditions, these intermediates undergo further condensation, aromatization, and carbonization, giving nanoscale sp^2-rich carbon domains decorated with oxygenated and nitrogen-containing surface groups. The proposed Amadori/Maillard-assisted formation pathway of glucose-derived GQDs is illustrated in Figure 1, showing the transformation of glucose and hexadecylamine into nitrogen-containing carbonaceous intermediates before hydrothermal carbonization into fluorescent GQDs.

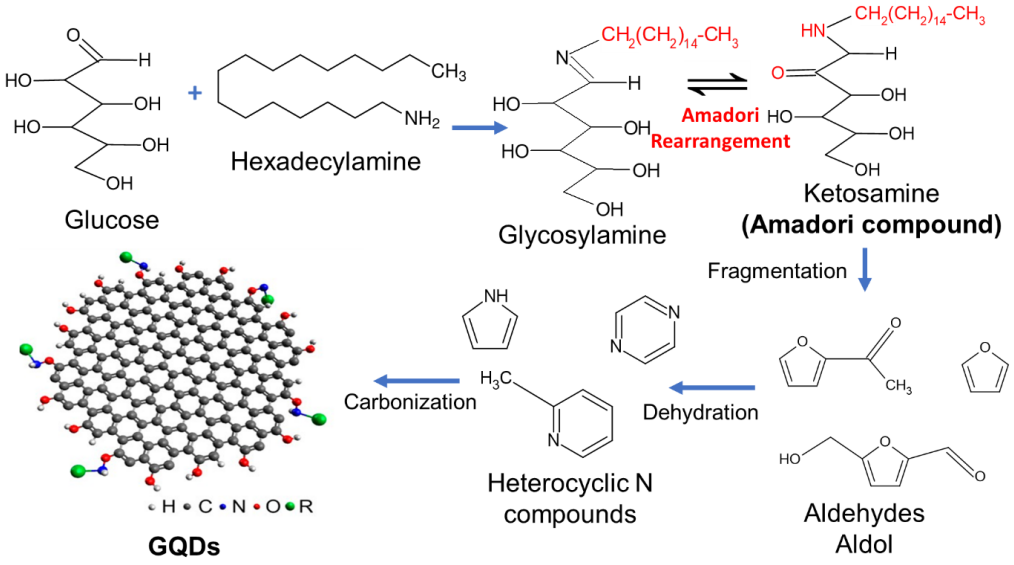

Figure 1. Proposed Amadori/Maillard-assisted formation route of glucose-derived graphene quantum dots (GQDs) in the presence of hexadecylamine and acetic acid

The role of acetic acid is not merely pH adjustment. In this synthesis, it supports the rearrangement and dehydration chemistry needed to convert glucose-derived intermediates into fluorescent carbonaceous domains. Hexadecylamine plays two roles: it supplies nitrogen-containing surface chemistry and can also act as a hydrophobic passivating agent that affects aggregation, hydrodynamic size, and fluorescence behavior. The cold methanol purification step is therefore critical; without efficient removal of residual long-chain amines, subsequent DLS and fluorescence data would be dominated by surfactant/amine aggregates rather than true GQD behavior (Lee *et al.*, 2019). The overall synthesis and purification workflow is summarized in Figure 2, covering precursor preparation, hydrothermal treatment, methanol-assisted quenching, cold-induced aggregation, filtration, and formation of a blue-luminescent GQD dispersion.

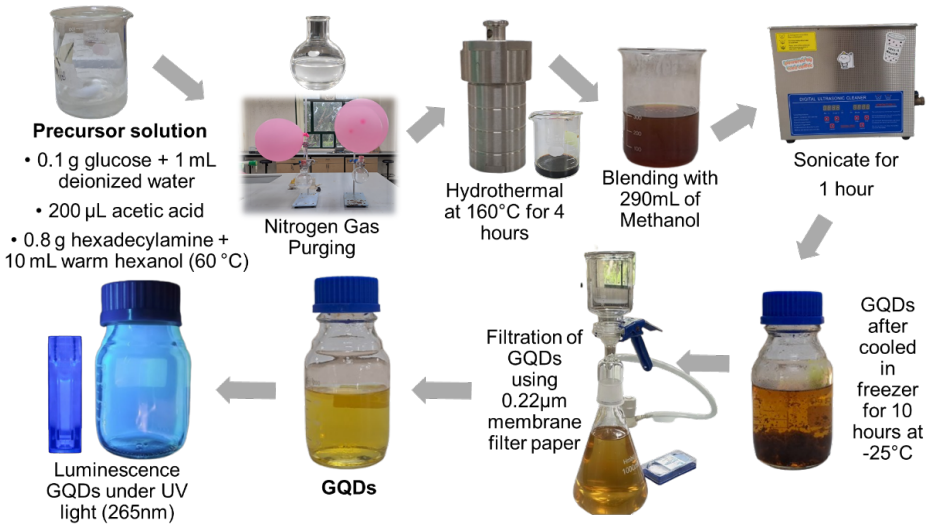

Figure 2. Schematic preparation and purification workflow for blue-luminescent graphene quantum dots (GQDs) synthesized from glucose

3.2. Surface functional groups characterization using ATR-FTIR

The ATR-FTIR spectrum of the synthesized GQDs is shown in Figure 3, and the corresponding peak assignments are summarized in Table 1. ATR-FTIR analysis confirmed that the synthesized GQDs were not bare carbon cores but surface-functionalized nanostructures. The broad band at 3,267 cm^{-1} was assigned primarily to N–H stretching, supporting the presence of amine-related groups introduced from hexadecylamine (Lee *et al.*, 2019). Peaks at 2,955 and 2,916 cm^{-1} corresponded to sp^3 C–H stretching, while the band at 2,849 cm^{-1} was assigned to sp^2 C–H stretching, indicating coexistence of aliphatic/passivating and graphitic/aromatic domains (Arthisree & Joshi, 2017). Bands at 1,638, 1,562, and 1,467 cm^{-1} were attributed to aromatic C=C stretching, with the 1,638 cm^{-1} region potentially overlapping with C=O stretching of carbonyl-containing groups (Önal *et al.*, 2019). The C–O band at 1,307 cm^{-1}, C–O–C band at 1,163 cm^{-1}, epoxide-related signal at 829 cm^{-1}, and C–H bending at 721 cm^{-1} confirm that oxygenated surface groups remained after hydrothermal carbonization.

These functional groups are central to the sensing concept. Oxygenated and amine-containing groups improve dispersibility and create binding or electrostatic interaction sites for bacterial cell-wall components. For *S. aureus*, a Gram-positive bacterium with a thick peptidoglycan layer and teichoic-acid-rich surface, such interactions may facilitate contact between the bacterial envelope and the fluorescent GQD surface. This contact can disturb excited-state recombination and promote fluorescence quenching, a mechanism commonly exploited in carbon-dot and GQD-based biosensing platforms (Bruce & Clapper, 2020; Li *et al.*, 2025; Luo *et al.*, 2021).

Table 1. ATR-FTIR peak assignments of synthesized GQDs

Wavenumber (cm^{-1})	Assignment
3,267	N–H stretching
2,955, 2,916	sp^3 C–H stretching
2,849	sp^2 C–H stretching
1,638	Aromatic C=C stretching / C=O stretching
1,562, 1,467	Aromatic C=C stretching
1,307	C–O stretching
1,163	C–O–C stretching
829	Epoxide ring stretching
721	In-plane and out-of-plane C–H bending

Abbreviations: ATR-FTIR: Attenuated total reflectance–Fourier transform infrared spectroscopy; GQD: Graphene quantum dot.

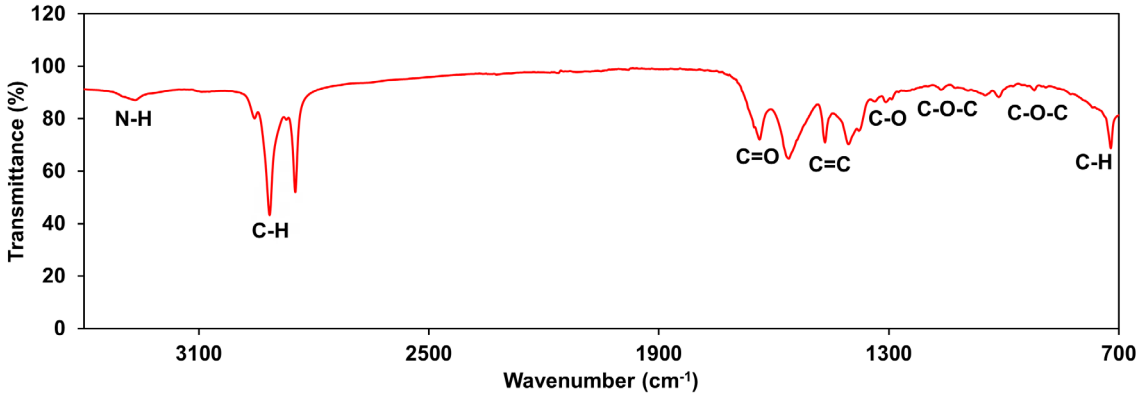

Figure 3. ATR-FTIR spectrum of synthesized GQDs showing amine, hydrocarbon, aromatic, carbonyl/oxygenated, and epoxide-related surface groups
Abbreviations: ATR-FTIR: Attenuated total reflectance–Fourier transform infrared spectroscopy; GQD: Graphene quantum dot.

3.3. Optical absorption behavior

The UV-Vis absorption spectrum of the synthesized GQDs is presented in Figure 4. The UV-Vis spectrum showed strong absorption in the ultraviolet region with peaks at 205 and 257 nm and a shoulder at approximately 340 nm. The 205 and 257 nm bands are assigned to π–π* transitions of sp^2-hybridized aromatic carbon domains, which are characteristic of graphitic carbon nanostructures (Tang *et al.*, 2012; Yang *et al.*, 2021; S. Zhu *et al.*, 2015). The shoulder around 340 nm is assigned to n–π* transitions associated with C=O and other oxygenated surface states. These absorption features support the conclusion that the hydrothermal product contained conjugated carbon domains with surface/edge states capable of UV excitation and blue emission.

The optical profile is consistent with the expected photoluminescence mechanism of GQDs, where emission can arise from a combination of quantum-confined sp^2 domains and surface/edge states (Wijayaratne *et al.*, 2022; S. Zhu *et al.*, 2017). The observed blue luminescence under UV irradiation suggests that the synthesized particles possess emissive states in the blue region, although the current dataset lacks full photoluminescence excitation-emission spectra and quantum-yield measurements. Therefore, the UV-Vis and visual fluorescence results are strong preliminary evidence, but publication-level optical claims should be strengthened by PL spectroscopy.

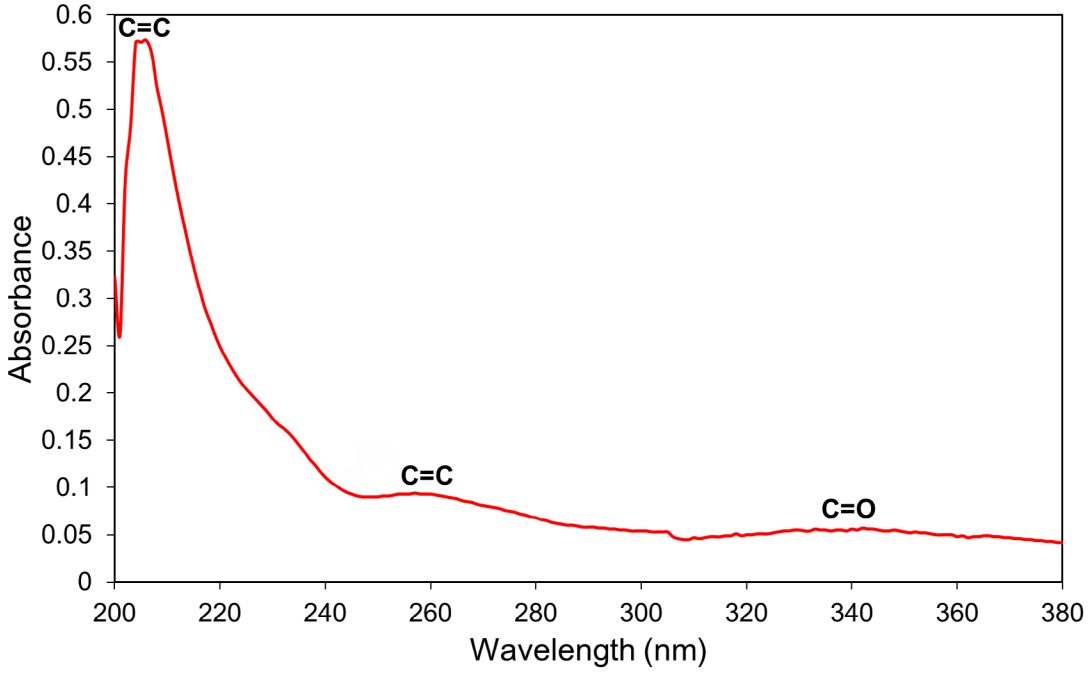

Figure 4. UV-Vis absorption spectrum of graphene quantum dots showing π–π* transitions of sp^2 carbon domains and an n–π* shoulder associated with oxygenated surface states

3.4. Particle-size distribution and morphology

The DLS particle-size distribution of the synthesized GQDs after ultrasonication is shown in Figure 5. DLS analysis after 2.5 h ultrasonication gave an average hydrodynamic diameter of 44.20 nm. Approximately 92.9% of the particles were distributed within the 0.1–1 μm range according to the DLS population output. This apparent mismatch between the average size and the broader population range is plausible because DLS measures hydrodynamic diameter rather than dry core diameter. For GQDs containing long-chain amine/passivating groups, the measured hydrodynamic size can include solvent layers, surface-bound molecules, and transient aggregates, all of which increase the apparent diameter relative to the TEM-observed core size (Azimi *et al.*, 2024).

The TEM micrographs and corresponding particle-size distribution histogram are shown in Figure 6. As shown in Figure 6a and 6b, the GQDs displayed a mostly spherical nanoscale morphology with some local agglomeration, while the particle-size distribution histogram in Figure 6c gave an estimated mean diameter of 33.69 nm. Individual particles measured from TEM images included particles of 28.38, 38.18, and 40.78 nm in more agglomerated regions and smaller particles of 21.41, 5.48, and 4.31 nm in more dispersed regions. The discrepancy between TEM and DLS is expected: TEM measures dried particles on a grid, while DLS measures solvated and possibly aggregated particles in dispersion. The data therefore indicate that the material is nanoscale and generally spherical, but the size distribution is broader than ideal for a high-impact sensing paper. Further purification, dialysis/size selection, and high-resolution TEM should be performed to determine the true GQD core size and crystallinity.

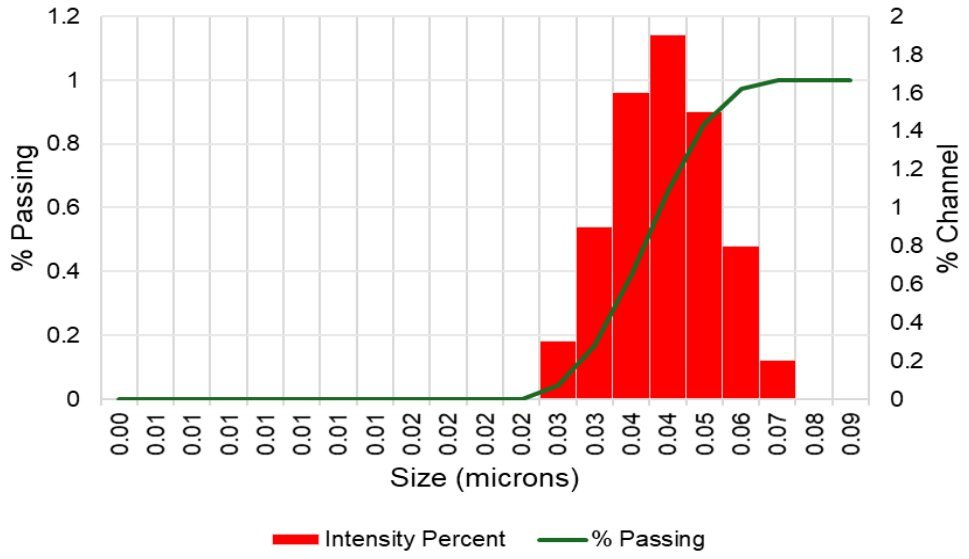

Figure 5. Dynamic light scattering particle-size distribution of synthesized graphene quantum dots after 2.5 h ultrasonication

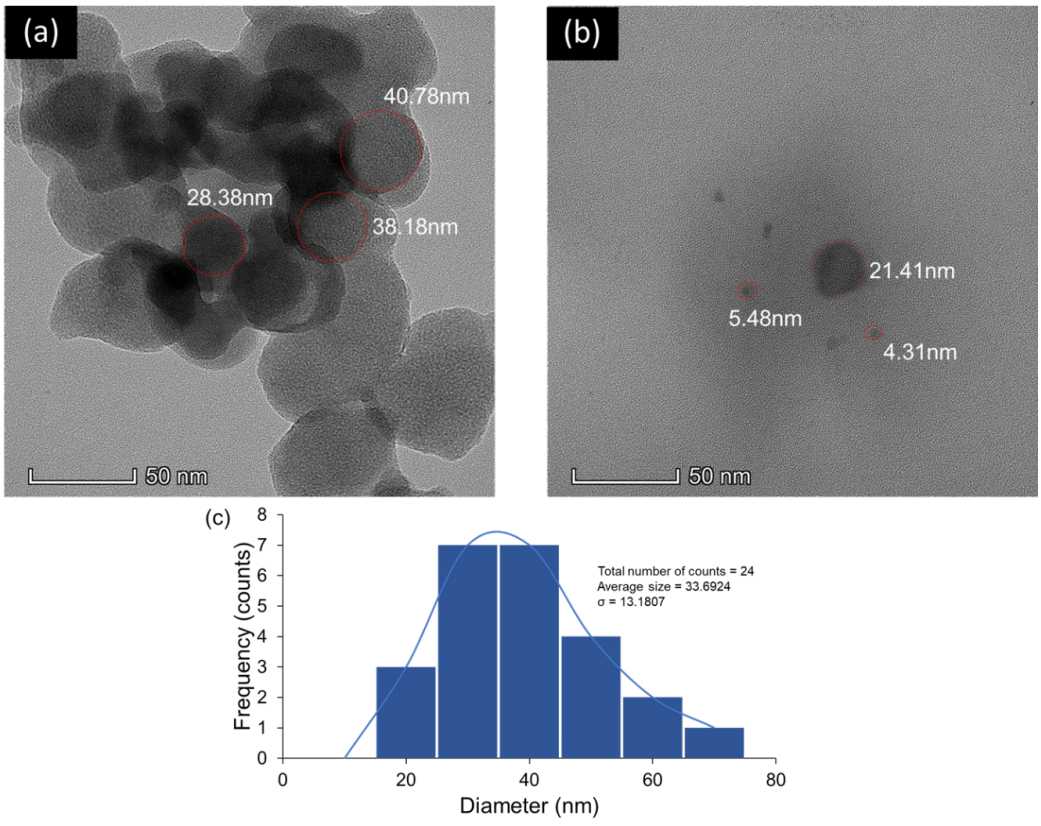

Figure 6. Transmission electron microscopy images of the synthesized GQDs at different regions (a, b) and corresponding particle-size distribution histogram (c), showing predominantly spherical particles with a mean diameter of 33.69 nm.

3.5. Smartphone-assisted fluorescence quenching response toward *Staphylococcus aureus*

The synthesized GQDs were evaluated as a turn-off fluorescent sensing probe for *S. aureus*. In a turn-off system, the fluorescence intensity of the probe decreases after interaction with the analyte, typically through static quenching, dynamic quenching, energy transfer, inner-filter effects, surface-state disruption, aggregation-induced quenching, or electron-transfer processes (Dehghani *et al.*, 2020; Ghanbarlou *et al.*, 2025; S. Zhu *et al.*, 2015). In the present system, the most reasonable preliminary interpretation is that *S. aureus* interacts with functional groups on the GQD surface, forming GQD–bacteria complexes that alter the emissive surface states and reduce fluorescence intensity. The ATR-FTIR evidence of N–H, C–O, C–O–C, epoxide, aromatic C=C, and carbonyl-related groups supports this surface-interaction mechanism. The proposed fluorescence-quenching mechanism between the functionalized GQDs and *S. aureus* is schematically illustrated in Figure 7.

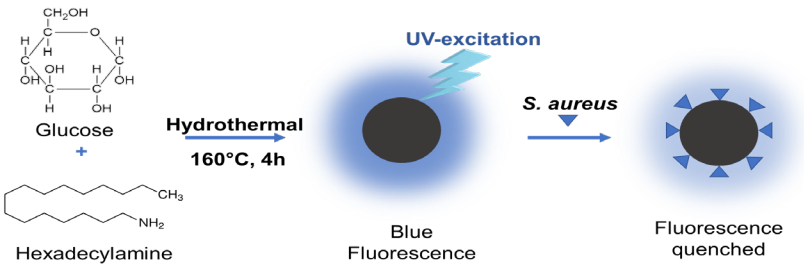

Figure 7. Schematic representation of GQD synthesis and proposed fluorescence-quenching mechanism upon interaction with *Staphylococcus aureus*

Smartphone-based imaging was used as a practical readout. The visual fluorescence response and the corresponding smartphone-based RGB/Stern–Volmer analysis are shown in Figure 8. The visual fluorescence images showed progressive quenching as the test concentration increased from 0.1 to 1.5 in the prepared series. RGB analysis gave a decreasing linear relationship for the R/(G+B) ratio, with $y = -0.0747x + 0.6186$ and $R^2 = 0.8218$. The Stern–Volmer-type F_0/F plot showed a stronger linear correlation with $R^2 = 0.9201$. These results suggest that GQDs respond to increasing *S. aureus* concentration with measurable fluorescence quenching and that smartphone-extracted color parameters can capture this trend. The fluorescence response observed in the GQD–*S. aureus* system indicates the feasibility of using the synthesized GQDs as smartphone-readable fluorescent probes for bacterial screening. However, the present evaluation should be interpreted as a proof-of-concept study rather than a fully validated quantitative diagnostic assay. Further work should include bacterial calibration using biologically meaningful concentration units such as colony-forming unit (CFU)/mL or optical density, appropriate blank and control systems, selectivity testing against non-target bacteria, determination of the limit of detection and limit of quantification, and validation in real food, water, or clinical matrices. These additional studies are necessary to establish the analytical reliability, selectivity, and practical applicability of the proposed sensing platform.

3.6. Comparison with existing bacterial sensing platforms

Compared with culture, enzyme-linked immunosorbent assay, and polymerase chain reaction, GQD-based optical sensing offers potential advantages in speed, portability, low reagent consumption, and compatibility with visual or smartphone readout (Awaludin *et al.*, 2020; Savas & Altintas, 2019; Zhao *et al.*, 2024). Reported GQD and carbon-dot platforms have achieved sensitive detection of *Escherichia coli* O157:H7, *Salmonella typhimurium*, *Leptospira interrogans*, and other bacteria using fluorescent, electrochemical, photoelectrochemical, immunoassay, and aptamer-assisted strategies (Castillo-Torres *et al.*, 2019; Jiang *et al.*, 2021; Xue *et al.*, 2020). The present platform is simpler because it avoids complex antibody or aptamer conjugation and uses image-based optical readout. This simplicity is valuable for low-resource screening, but it also creates a selectivity weakness because label-free fluorescence quenching can be caused by many cells, proteins, salts, pH changes, or matrix interferents.

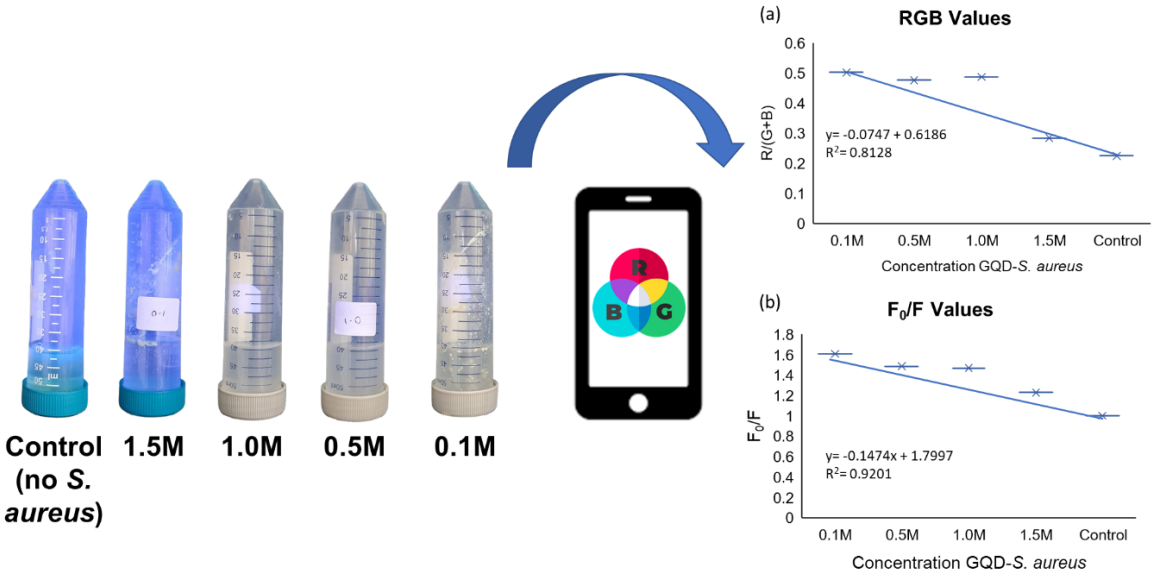

Figure 8. Visual fluorescence response of graphene quantum dot–*Staphylococcus aureus* samples and smartphone-based RGB/Stern–Volmer analysis. (a) RGB values. (b) F_0/F values.

The present study demonstrates a low-cost and practical fluorescence detection platform based on glucose-derived GQDs synthesized through an Amadori-assisted hydrothermal route, followed by cold-aggregation purification and smartphone-assisted fluorescence analysis. The synthesized GQDs exhibited blue fluorescence, surface functional groups suitable for bacterial interaction, and nanoscale morphology, supporting their preliminary applicability as fluorescent probes for *S. aureus* detection. Nevertheless, further validation is required to establish the system as a fully optimized bacterial sensor. Future work should include calibration using bacterial concentration in CFU/mL, determination of the limit of detection and limit of quantification, selectivity studies against non-target bacterial species, reproducibility and stability assessment, and recovery studies in real food, water, or clinical matrices.

4. Conclusion

Blue-luminescent GQDs were successfully synthesized from glucose through an Amadori-rearrangement-assisted hydrothermal route using hexadecylamine and acetic acid. ATR-FTIR confirmed the presence of amine, aromatic, hydrocarbon, carbonyl/oxygenated, C–O, C–O–C, and epoxide-related surface groups, while UV-Vis spectroscopy showed characteristic π–π^* transitions at 205 and 257 nm and an n–π^* shoulder near 340 nm. DLS gave an average hydrodynamic diameter of 44.20 nm, whereas TEM confirmed predominantly spherical nanoscale particles with an estimated mean diameter of 33.69 nm. The synthesized GQDs exhibited fluorescence quenching in the presence of *S. aureus*, and smartphone-based RGB analysis produced measurable concentration-dependent responses, including an R/(G+B) correlation with R^2 = 0.8218 and a Stern–Volmer-type F_0/F correlation with R^2 = 0.9201. These findings demonstrate the feasibility of glucose-derived blue-luminescent GQDs as low-cost fluorescent nanoprobes for smartphone-assisted screening of *S. aureus*. Further validation using calibrated CFU/mL bacterial concentrations, photoluminescence spectroscopy, selectivity studies against non-target bacteria, reproducibility assessment, limit of detection/limit of quantification determination, and real-sample analysis is required to develop this proof-of-concept system into a quantitative bacterial sensing platform.

Acknowledgements

The authors gratefully acknowledge the Department of Chemistry, Kulliyyah of Science, International Islamic University Malaysia, for providing laboratory facilities and technical support.

Funding

This work was supported by MIMOS Berhad through a consultancy project.

Conflict of interest

The authors declare no competing interests.

Ethical approval

Not applicable. This study did not involve human participants or animal experiments.

Data availability

All data generated or analyzed during this study are included in this article.

Author contributions

Siti Nor Hadijah Zalriadi: Writing - original draft preparation, Methodology, Investigation, Formal analysis; Siti Aisyah Saiful Adlee: Methodology, Investigation, Writing – review and editing; Wan Hazman Danial: Methodology, Investigation, Conceptualization, Writing – review and editing, Supervision, Validation; Mohammad Norazmi Ahmad: Supervision, Validation.

References

Arthisree, D., & Joshi, G. M. (2017). Study of Polymer Graphene Quantum Dot Nanocomposites. *Journal of Materials Science: Materials in Electronics*, *28*(14), 10516–10524.

https://doi.org/10.1007/s10854-017-6825-6

Awaludin, N., Abdullah, J., Salam, F., Ramachandran, K., Yusof, N. A., & Wasoh, H. (2020). Fluorescence-based Immunoassay for the Detection of Xanthomonas Oryzae Pv. Oryzae in Rice Leaf. *Analytical Biochemistry*, *610*, 113876.

https://doi.org/10.1016/j.ab.2020.113876

Azimi, Z., Alimohammadian, M., & Sohrabi, B. (2024). Graphene Quantum Dots Based on Mechanical Exfoliation Methods: A Simple and Eco-Friendly Technique. *ACS Omega*, *9*(29), 31427–31437.

https://doi.org/10.1021/acsomega.4c00453

Bressi, V., Ferlazzo, A., Iannazzo, D., & Espro, C. (2021). Graphene Quantum Dots by Eco-friendly Green Synthesis for Electrochemical Sensing: Recent Advances and Future Perspectives. *Nanomaterials*, *11*(5), 1120.

https://doi.org/10.3390/nano11051120

Bruce, J. A., & Clapper, J. C. (2020). Conjugation of Carboxylated Graphene Quantum Dots with Cecropin P1 for Bacterial Biosensing Applications. *ACS Omega*, *5*(41), 26583–26591.

https://doi.org/10.1021/acsomega.0c03342

Castillo-Torres, K. Y., Arnold, D. P., & McLamore, E. S. (2019). Rapid Isolation of Escherichia coli from Water Samples Using Magnetic Microdiscs. *Sensors and Actuators B: Chemical*, *291*, 58–66.

https://doi.org/10.1016/j.snb.2019.04.043

Chen, W., Lv, G., Hu, W., Li, D., Chen, S., & Dai, Z. (2018). Synthesis and Applications of Graphene Quantum Dots: A review. *Nanotechnology Reviews*, *7*(2), 157–185.

https://doi.org/10.1515/ntrev-2017-0199

Cho, S., Kim, H., Song, D., Jung, J., Park, S., Jo, H., Seo, S., Han, C., Park, S., Kwon, W., & Han, H. (2024). Insights into Glucose-derived Carbon Dot Synthesis via Maillard Reaction: From Reaction Mechanism to Biomedical Applications. *Scientific Reports*, *14*(1), 31325.

https://doi.org/10.1038/s41598-024-82767-z

Danial, W. H., Abdullah, M., Abu Bakar, M. A., Yunos, M. S., Ibrahim, A. R., Iqbal, A., & Adnan, N. N. (2022). The valorisation of Grass Waste for the Green Synthesis of Graphene Quantum Dots for Nonlinear Optical Applications. *Optical Materials*, *132*, 112853.

https://doi.org/10.1016/j.optmat.2022.112853

Dehghani, Z., Mohammadnejad, J., Hosseini, M., Bakhshi, B., & Rezayan, A. H. (2020). Whole cell FRET Immunosensor Based on Graphene Oxide and Graphene Dot for Campylobacter Jejuni Detection. *Food Chemistry*, *309*, 125690.

https://doi.org/10.1016/j.foodchem.2019.125690

Elvati, P., Baumeister, E., & Violi, A. (2017). Graphene Quantum Dots: Effect of Size, Composition and Curvature on Their Assembly. *RSC Advances*, *7*(29), 17704–17710.

https://doi.org/10.1039/c7ra01029j

Fu, W., Ling, M., Fu, X., Wang, L., Xu, S., Wang, G., Liu, R., Han, C., Li, G., Zhang, J., Liu, Z., & Jin, J. (2024). Green Synthesized Nitrogen-doped Carbon Quantum Dots for Fluorescence Sensing, Information Encryption and Smartphone-assisted Visual Detection. *Dyes and Pigments*, *231*, 112394.

https://doi.org/10.1016/j.dyepig.2024.112394

Ghanbarlou, S., Kahforoushan, D., Abdollahi, H., Zarrintaj, P., Alomar, A., Villanueva, C., & Davachi, S. M. (2025). Advances in Quantum Dot-based Fluorescence Sensors for Environmental and Biomedical Detection. *Talanta*, *294*, 128176.

https://doi.org/10.1016/j.talanta.2025.128176

Girma, A. (2025). Staphylococcus aureus: Current Perspectives on Molecular Pathogenesis and Virulence. *Cell Surface*, *13*, 100137.

https://doi.org/10.1016/j.tcsw.2024.100137

Haag, A. F., Fitzgerald, J. R., & Penadés, J. R. (2019). Staphylococcus aureus in Animals. *Microbiology Spectrum*, *7*(3).

https://doi.org/10.1128/microbiolspec.gpp3-0060-2019

Jiang, D., Du, X., Liu, Q., Zhou, L., Dai, L., Qian, J., Wang, K., & Qiu, B. (2021). Silver Nanoparticle-anchored WO3 Nanosheets and Nitrogen-doped Graphene Quantum Dots for Enhanced Photoelectrochemical Detection of Escherichia coli O157:H7. *Biosensors and Bioelectronics*, *183*, 113214.

https://doi.org/10.1016/j.bios.2021.113214

Kalluri, A., Debnath, D., Dharmadhikari, B., & Patra, P. (2018). Graphene Quantum Dots: Synthesis and Applications. *Methods in Enzymology*, *609*, 335–354.

https://doi.org/10.1016/bs.mie.2018.06.006

Kalkal, A., Pradhan, R., Kadian, S., Manik, G., Packirisamy, G. (2020). Biofunctionalized Graphene Quantum Dots Based Fluorescent Biosensor Toward Efficient Detection of Small Cell Lung Cancer. *ACS Applied Bio Materials*, *3*(8), 4922–4932.

https://doi.org/10.1021/acsabm.0c00427

Kwon, S., Jamal, H., Choi, J., Park, H., Song, J., & Lee, C. (2022). Synthesis and characterization of graphene quantum dot/SiNP/carbon nanomaterial composites. *Applied Nanoscience*, *12*(11), 3219–3228.

https://doi.org/10.1007/s13204-022-02676-3

Lee, S. H., Kim, D. Y., Lee, J., Lee, S. B., Han, H., Kim, Y. Y., Mun, S. C., Im, S. H., Kim, T. H., & Park, O. O. (2019). Synthesis of Single-Crystalline Hexagonal Graphene Quantum Dots from Solution Chemistry. *Nano Letters*, *19*(8), 5437–5442.

https://doi.org/10.1021/acs.nanolett.9b01940

Liu, C., Geng, Q., & Geng, Z. (2024). Strategies to Improve Performances of Fluorescent Biosensors Based on Smartphones: Sensitivity, High Throughput, and Smart Detection. *Sensors and Actuators A: Physical*, *368*, 115120.

https://doi.org/10.1016/j.sna.2024.115120

Li, K., Fang, S., Wu, T., Zheng, C., Zeng, Y., He, J., Zhang, Y., & Lu, Z. (2025). Aptamer-functionalized Graphene Quantum Dots Combined with Artificial Intelligence Detect Bacteria for Urinary Tract Infections. *Frontiers in Cellular and Infection Microbiology*, *15*, 1555617.

https://doi.org/10.3389/fcimb.2025.1555617

Luo, Y., Liu, F., Song, J., Luo, Q., Yang, Y., Mei, C., Xu, M., & Liao, B. (2021). Function-Oriented Graphene Quantum Dots Probe for Single Cell in situ Sorting of Active Microorganisms in Environmental Samples. *Frontiers in Microbiology*, *12*, 659111.

https://doi.org/10.3389/fmicb.2021.659111

Mielewczyk, L., Liebscher, V., Grothe, J., & Kaskel, S. (2025). Green Synthesis of Copper Nanoparticles utilising the Maillard Reaction. *Chemistry - A European Journal*, *31*, e202404314.

https://doi.org/10.1002/chem.202404314

Mlynarczyk-Bonikowska, B., & Rudnicka, L. (2025). The Pathogenicity Mechanisms of Staphylococcus aureus. *International Journal of Molecular Sciences*, *26*(24), 11803.

https://doi.org/10.3390/ijms262411803

Moellering, R. C. (2010). MRSA: The first half century. *Journal of Antimicrobial Chemotherapy*, *67*(1), 4–11.

https://doi.org/10.1093/jac/dkr437

Mohammad Ameen, S. S., Algethami, F. K., & Omer, K. M. (2025). Triple-color Emission Ratiometric Fluorescence in Biochemical Sensing Analysis; Principles, Probe Fabrication and Applications. *TrAC - Trends in Analytical Chemistry*, *193*, 118489.

https://doi.org/10.1016/j.trac.2025.118489

Önal, Y., Kır, Ş., Dehri, İ., & Esen, R. J. (2019). Synthesis and Characterization of Graphene Quantum Dots From Dried Pine Leaves. *International Journal of Scientific and Technological Research*, *2*(2), 109–120. https://izlik.org/JA54DB49ZU

Padmavathi, B., & Vijayakumar, V. (2023). Green Synthesis, Characterisation, Optical Properties of Graphene Quantum Dots with Anti Bacterial Characteristics. *Optical and Quantum Electronics*, *55*(12), 1109.

https://doi.org/10.1007/s11082-023-05396-2

Qu, D., Zheng, M., Zhang, L., Zhao, H., Xie, Z., Jing, X., Haddad, R. E., Fan, H., & Sun, Z. (2014). Formation mechanism and optimization of highly luminescent N-doped graphene quantum dots. *Scientific Reports*, *4*, 5294.

https://doi.org/10.1038/srep05294

Rasheed, P. A., Ankitha, M., Pillai, V. K., & Alwarappan, S. (2024). Graphene Quantum Dots for Biosensing and Bioimaging. *RSC Advances*, *14*(23), 16001–16023.

https://doi.org/10.1039/d4ra01431f

Roh, S. G., Robby, A. I., Phuong, P. T. M., In, I., & Park, S. Y. (2019). Photoluminescence-tunable Fluorescent Carbon Dots-deposited Silver Nanoparticle for Detection and Killing of Bacteria. *Materials Science and Engineering C*, *97*, 613–623.

https://doi.org/10.1016/j.msec.2018.12.070

Rosato, R., Santarelli, G., Augello, A., Perini, G., de Spirito, M., Sanguinetti, M., Papi, M., & de Maio, F. (2024). Exploration of the Graphene Quantum Dots-Blue Light Combination: A Promising Treatment against Bacterial Infection. *International Journal of Molecular Sciences*, *25*(15), 8033.

https://doi.org/10.3390/ijms25158033

Savas, S., & Altintas, Z. (2019). Graphene Quantum Dots as Nanozymes for Electrochemical Sensing of Yersinia enterocolitica in Milk and Human Serum. *Materials*, *12*(13), 2189.

https://doi.org/10.3390/ma12132189

Shebeeb, C. M., Joseph, A., Farzeena, C., Dinesh, R., & Sajith, V. (2022). Fluorescent carbon dot embedded polystyrene particle: an alternative to fluorescently tagged polystyrene for fate of microplastic studies: a preliminary investigation. *Applied Nanoscience*, *12*(9), 2725–2731.

https://doi.org/10.1007/s13204-022-02566-8

Shi, L., Wang, B., & Lu, S. (2023). Efficient Bottom-up Synthesis of Graphene Quantum Dots at an Atomically Precise Level. *Matter*, *6*(3), 728–760.

https://doi.org/10.1016/j.matt.2023.01.003

Sun, F., Ghosh, H., Tan, Z., & Sivoththaman, S. (2023). Top-down Synthesis and Enhancing Device Adaptability of Graphene Quantum Dots. *Nanotechnology*, *34*(18), 185601.

https://doi.org/10.1088/1361-6528/acb7fb

Šuster, K., & Cör, A. (2023). Induction of Viable but Non-Culturable State in Clinically Relevant Staphylococci and Their Detection with Bacteriophage K. *Antibiotics*, *12*(2), 311.

https://doi.org/10.3390/antibiotics12020311

Tang, L., Ji, R., Cao, X., Lin, J., Jiang, H., Li, X., Teng, K. S., Luk, C. M., Zeng, S., Hao, J., & Lau, S. P. (2012). Deep Ultraviolet Photoluminescence of Water-soluble Self-passivated Graphene Quantum Dots. *ACS Nano*, *6*(6), 5102–5110.

https://doi.org/10.1021/nn300760g

Wang, Y., Dai, S., Guo, J., Wang, Y., & Tang, B. (2025). A Facile Synthesis Strategy for N-Doped Graphene Quantum Dots Electrode Materials: Electrochemical Behaviors and Universal Energy Storage Mechanism. *Materials*, *18*(23), 5373.

https://doi.org/10.3390/ma18235373

Wijayaratne, K., Thennakoon, T. M. A. A. B., & Bandara, T. M. W. J. (2022). Graphene Quantum Dot (GQD) Synthesis: A Review of the Methods, Challenges and Future Prospects. *Ceylon Journal of Science*, *51*(3), 195–207.

https://doi.org/10.4038/cjs.v51i3.8028

Xue, L., Huang, F., Hao, L., Cai, G., Zheng, L., Li, Y., & Lin, J. (2020). A Sensitive Immunoassay for Simultaneous Detection of Foodborne Pathogens Using MnO2 Nanoflowers-assisted Loading and Release of Quantum Dots. *Food Chemistry*, *322*, 126719.

https://doi.org/10.1016/j.foodchem.2020.126719

Yang, P. C., Ting, Y. X., Gu, S., Gandomi, Y. A., Li, J., & Hsieh, C. te. (2021). Effect of Solvent on Fluorescence Emission From Polyethylene Glycol-coated Graphene Quantum Dots Under Blue Light Illumination. *Nanomaterials*, *11*(6), 1383.

https://doi.org/10.3390/nano11061383

Zhang, J., Xia, A., Chen, H., Nizami, A. S., Huang, Y., Zhu, X., Zhu, X., & Liao, Q. (2022). Biobased Carbon Dots Production via Hydrothermal Conversion of Microalgae Chlorella Pyrenoidosa. *Science of the Total Environment*, *839*, 156144.

https://doi.org/10.1016/j.scitotenv.2022.156144

Zhao, X., Bhat, A., O'Connor, C., Curtin, J., Singh, B., & Tian, F. (2024). Review of Detection Limits for Various Techniques for Bacterial Detection in Food Samples. *Nanomaterials*, *14*(10), 855.

https://doi.org/10.3390/nano14100855

Zhu, S., Song, Y., Zhao, X., Shao, J., Zhang, J., & Yang, B. (2015). The Photoluminescence Mechanism in Carbon Dots (Graphene Quantum Dots, Carbon Nanodots, and Polymer Dots): Current State and Future Perspective. *Nano Research*, *8*(2), 355–381.

https://doi.org/10.1007/s12274-014-0644-3

Zhu, S., Song, Y., Wang, J., Wan, H., Zhang, Y., Ning, Y., & Yang, B. (2017). Photoluminescence Mechanism in Graphene Quantum Dots: Quantum Confinement Effect and Surface/Edge State. *Nano Today*, *13*, 10–14.

https://doi.org/10.1016/j.nantod.2016.12.006

Zhu, Z., Hu, Z., Li, S., Fang, R., Ono, H. K., & Hu, D. L. (2024). Molecular Characteristics and Pathogenicity of Staphylococcus aureus Exotoxins. *International Journal of Molecular Sciences*, *25*(1), 395.

https://doi.org/10.3390/ijms25010395